

# Substituent Effects on Photosensitized Splitting of Thymine Cyclobutane Dimer by an Attached Indole

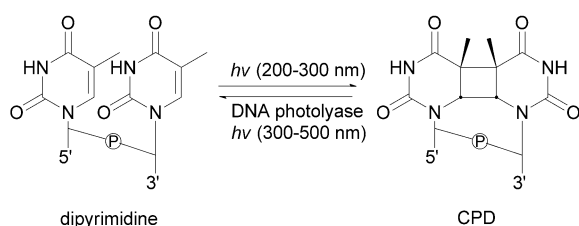
Wenjian Tang,<sup>\*,[a]</sup> Hongmei Zhou,<sup>[a]</sup> Jing Wang,<sup>[a]</sup> Chunxiao Pan,<sup>[a]</sup> Jingbo Shi,<sup>[a]</sup> and Qinhua Song<sup>\*,[b]</sup>

In chromophore-containing cyclobutane pyrimidine dimer (CPD) model systems, solvent effects on the splitting efficiency may depend on the length of the linker, the molecular conformation, and the oxidation potential of the donor. To further explore the relationship between chromophore structure and splitting efficiency, we prepared a series of substituted indole-T< >T model compounds **2a–2g** and measured their splitting quantum yields in various solvents. Two reverse solvent effects were observed: an increase in splitting efficiency in solvents of lower polarity for models **2a–2d** with an electron-donating group (EDG), and vice versa for models **2e–2g** with an electron-withdrawing group (EWG). According to the Hammett

equation, the negative value of the slope of the Hammett plot indicates that the indole moiety during the T< >T-splitting reaction loses negative charge, and the larger negative value implies that the repair reaction is more sensitive to substituent effects in low-polarity solvents. The EDGs of the models **2a–2d** can delocalize the charge-separated state, and low-polarity solvents make it more stable, which leads to higher splitting efficiency in low-polarity solvents. Conversely, the EWGs of models **2e–2g** favor destabilization of the charge-separated state, and high-polarity solvents decrease the destabilization and hence lead to more efficient splitting in high-polarity solvents.

## 1. Introduction

A type of major damage to DNA caused by UV irradiation is the formation of base photolesions, which may be mutagenic and are a leading cause of skin cancer.<sup>[1,2]</sup> The most frequent of these UV-induced lesions in DNA are cyclobutane pyrimidine dimers (CPDs), formed by [2+2] cycloaddition of two adjacent pyrimidine bases, more frequently thymines (Scheme 1). CPDs are specifically recognized and repaired by CPD photolyase, a single  $\approx 55$  kDa protein found in organisms from all king-



**Scheme 1.** UV-induced CPD photoproducts in DNA and their photorepair by DNA photolyases.

doms of life, except for placental mammals such as humans, which remove CPD lesions through nucleotide excision repair.<sup>[3]</sup> Experimental<sup>[4]</sup> and theoretical<sup>[5]</sup> investigations have provided evidence for the mechanisms of CPD photolyases. The enzymes transfer light energy, initially absorbed by an auxiliary chromophore, to a reduced flavin adenine dinucleotide (FADH<sup>-</sup>) coenzyme. The excited FADH<sup>-</sup> then transfers an electron to the CPD lesion, which subsequently leads to stepwise splitting of the C5–C5' and C6–C6' bonds and thus to transfor-

mation of the thymine dimer into the original bases. Formation of the repaired thymine monomers is finally followed by back electron transfer to produce the FADH<sup>•</sup> radical and thus restore the functional form of flavin for a new cycle of catalysis.

Some model compounds<sup>[6–8]</sup> that mimic the action of CPD photolyase have been designed, such as a chromophore attached to a CPD unit. Studies performed with these compounds have offered useful insights into the electron-transfer and bond-breaking processes involved in photosensitized CPD splitting. In the chromophore-containing CPD model systems, the splitting efficiency of the CPD units displays two reverse solvent effects. One is faster splitting in low polarity solvents,<sup>[9]</sup> which has been interpreted in terms of possible slowing of the highly exothermic back electron transfer process due to Marcus-region inverted behavior. The other is faster splitting in higher polarity solvents.<sup>[10]</sup> Recently, several model systems

[a] Dr. W. J. Tang, H. M. Zhou, J. Wang, C. X. Pan, Dr. J. B. Shi  
School of Pharmacy  
Anhui Medical University  
Hefei 230032 (China)  
Fax: (+86) 551-5161115  
E-mail: tangwjster@gmail.com

[b] Prof. Q. H. Song  
Department of Chemistry  
University of Science and Technology of China  
Hefei 230026 (China)  
Fax: (+86) 551-3601592  
E-mail: qhsong@ustc.edu.cn

Supporting information for this article is available on the WWW under <http://dx.doi.org/10.1002/cphc.201200652>.

were devised to explore the origin of these two reverse solvent effects.<sup>[11, 12]</sup>

In the indole–CPD model systems with different-length linkers,<sup>[11]</sup> the solvent effect on CPD splitting for model compounds with a long and flexible linker was just the reverse of that with a short linker, due to the much shorter distance between the indole and CPD owing to spreading to a U-shaped conformation with increasing solvent polarity because of their hydrophobic interaction and the specific structure of the CPD. However, our recent research<sup>[12b]</sup> showed that in the chromophore-containing CPD model systems with a short linker, the solvent effect of CPD splitting in phenothiazine model systems was contrary to that in non-phenothiazine model systems. The same phenomenon was also observed in two classes of model systems:<sup>[12a]</sup> covalently linked CPD– and oxetane–carbazole compounds with the same short linker. Whether in CPD– and oxetane–carbazole systems with the same linker and electron donor or in chromophore-containing CPD systems with the same linker and electron acceptor, a lower redox potential should be a key factor leading to back electron transfer lying in the different Marcus regions and the two reverse solvent effects. Therefore, many factors influence the solvent dependence of the splitting quantum yields, such as the length of the linker, the molecular conformation, the redox potential, and so on.

To further explore the relationship between chromophore structure and CPD splitting, we prepared a series of covalently linked indole cyclobutane thymine dimer (T<>T) model compounds with different substituents **2a–2g**, and investigated the solvent dependence of the T<>T splitting efficiency in various solvents. Although trimethylene-bridged T<>T enforces an almost planar ring, which is different to that of the unbridged T<>T, the bridged T<>T displays similar splitting efficiency.<sup>[10c, 13]</sup> The quantum yields of the T<>T splitting exhibited two reverse solvent effects: an increase in the splitting efficiency in low-polarity solvents for model compounds with an EDG (**2a–2d**), and faster splitting in higher polarity solvents for those with an EWG (**2e–2g**). The experimental results were analyzed by using the Hammett equation.<sup>[14]</sup> Furthermore, based on the solvent effects and the substituent effects on T<>T splitting, some new insights into the intramolecular electron-transfer process in indole–T<>T model systems were gained (Figure 1)

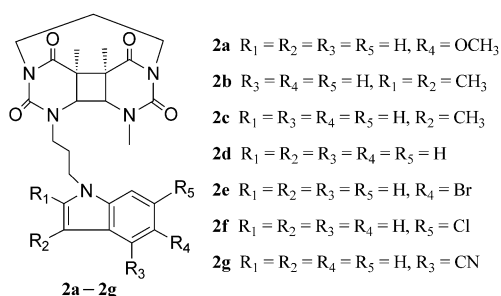


Figure 1. Chemical structure of model compounds with a short linker.

## 2. Results and Discussion

The photophysical and photochemical processes of model compounds **2a–2g** (represented as Ch–D) are illustrated by a simple mechanistic scheme (Figure 2).<sup>[10]</sup> Under irradiation by

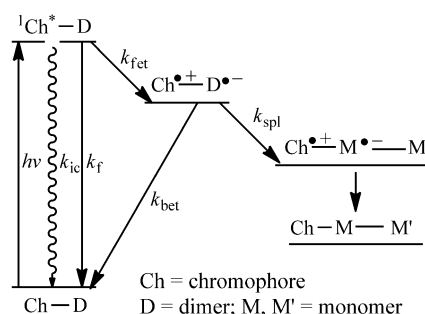


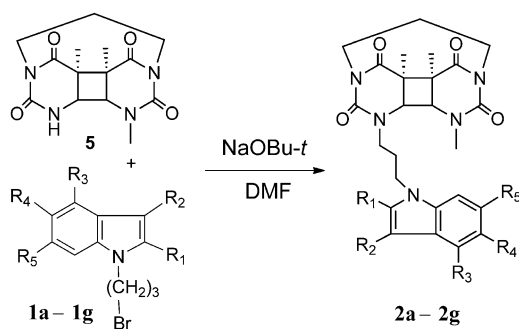
Figure 2. Photophysical and photochemical processes of the model compounds.

light with wavelengths above 290 nm, the chromophore moiety absorbs a photon, producing the excited state ( $^1\text{Ch}^*-\text{D}$ ). This excited state has the following relaxation pathways: fluorescence ( $k_f$ ), internal conversion ( $k_{ic}$ ), and electron transfer to the linked T <> T ( $k_{fet}$ ). The charge-separated species

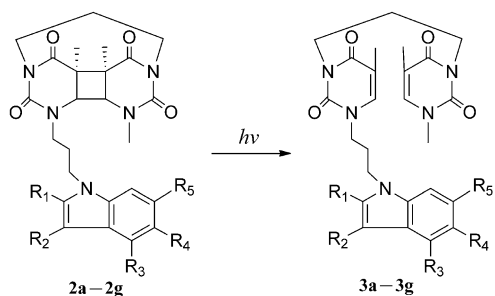
( $\text{Ch}^+-\text{D}^-$ ) formed by electron transfer undergoes two competitive processes: T <> T splitting ( $k_{spl}$ ) to produce  $\text{M}'$  and  $\text{Ch}^+-\text{M}'$ , which then becomes  $\text{Ch}-\text{M}$  by charge combination, and back electron transfer ( $k_{bet}$ ) resulting in an unproductive reversal. These processes undoubtedly have counterparts in the enzymatic repair process. In these processes,  $k_{fet}$  and  $k_{spl}$  contribute to the observed splitting quantum yield  $\Phi$  of T <> T splitting, while  $k_{bet}$ ,  $k_f$ , and  $k_{ic}$  would reduce the quantum efficiency. Back electron transfer is a key factor leading to low splitting efficiencies in model systems, but can be efficiently suppressed in CPD photolyases with a uniformly high repair efficiency ( $\Phi = 0.7-0.98$ ).<sup>[3]</sup> Besides, internal conversion ( $k_{ic}$ ) and the molecular conformation play important roles in resulting in a low splitting efficiency.<sup>[15]</sup>

To investigate the mechanisms of the above photoinduced electron-transfer processes, seven model compounds **2a–2g** with different substituted indoles and a short (trimethylene) linker between the chromophore and T <> T were synthesized as shown in Scheme 2. Model compounds **2a–2g** were prepared from the *cis-syn* thymine dimer<sup>[11]</sup> **5** alkylated with the corresponding 1-(3-bromopropyl)indole or its derivatives **1a–1g** (Scheme 2). The *N*-alkylation of indole or its derivative with an excess of 1,3-dibromopropane was carried with tetrabutylammonium bromide (TBAB) as phase-transfer catalyst in toluene/water.

The splitting properties of these model compounds were investigated in solvents of different polarity. After UVB irradiation of **2a–2g** in methanol solutions with the corresponding monochromatic light, analysis of the photolysis mixture by reversed-phase HPLC confirmed that the model compounds react cleanly to give **3a–3g**, respectively, as no other products could be detected besides the expected photoproducts (Scheme 3).



Scheme 2. Synthesis of model compounds.



Scheme 3. Photosensitized splitting reactions of the T &lt; &gt; T unit of the model compounds under irradiation with an appropriate wavelength of light.

To measure the splitting quantum yields  $\Phi$  of the model compounds, sample solutions were prepared in solvents of different polarity [THF, acetonitrile, methanol, and water/THF (25/75, 50/50, 75/25, 90/10)], placed in cuvettes with a Teflon stopper, and then irradiated with monochromatic light from a fluorescence spectrometer. After certain time intervals, the absorption spectra of the irradiated solutions were recorded with a

UV/Vis spectrometer. The intensity of irradiation light was measured three times during the measurement, and the average of three measurements was employed to obtain a value. Based on these data, the quantum yields of the splitting of the model compounds were obtained and are listed in Table 1.

The data in Table 1 show that the quantum yields for T < > T splitting of models 2a–2g are strongly solvent dependent and that the solvent effect on splitting efficiency varies

Table 1. Splitting quantum yields  $\Phi^{[a]}$  of model compounds 2a–2g in various solvents.

Solvent	2a	2b	2c	2d	2e	2f	2g
THF/H <sub>2</sub> O (10/90)	0.113	0.073	0.098	0.095	0.080	0.073	0.083
THF/H <sub>2</sub> O (25/75)	0.146	0.101	0.130	0.123	0.061	0.061	0.033
THF/H <sub>2</sub> O (50/50)	0.169	0.130	0.153	0.131	0.028	0.026	0.008
THF/H <sub>2</sub> O (75/25)	0.192	0.131	0.156	0.145	0.013	0.015	0.005
MeCN	0.184	0.157	0.153	0.147	0.012	0.012	0.002
MeOH	0.213	0.162	0.171	0.181	0.042	0.038	0.004
THF	0.180	0.153	0.153	0.219	0.014	0.005	– <sup>[b]</sup>

[a] Average of two determinations, experimental error  $\pm 5\%$ . [b] No splitting detected.

with the substituent. The splitting quantum yield shows a normal relation with solvent polarity for the model compounds with an EWG (2e–2g), but an inverse relation for the model compounds with an EDG (2a–2d). Therefore, in model compounds 2a–2g with a short linker, those with an EDG show a contrary solvent effect to those with an EWG.

The two reverse solvent effects on the splitting efficiency observed previously in different model systems<sup>[11,12]</sup> may be due to the length of the linker, the molecular conformation, the oxidation potential of donor, and so on. For the covalently linked chromophore–dimer systems, fluorescence quenching efficiency  $Q$  of the chromophore can reflect the efficiency of forward electron transfer ( $Q = \phi_{\text{red}}$ ).<sup>[10]</sup> Data in Table 2 show that

Table 2. Extent of fluorescence quenching ( $Q$ ) of model compounds 2a–2g in various solvents<sup>[a]</sup>.

Solvent	2a	2b	2c	2d	2e	2f	2g
THF/H <sub>2</sub> O (10/90)	0.85	0.94	0.74	0.90	0.74	0.75	0.36
THF/H <sub>2</sub> O (25/75)	0.70	0.96	0.82	0.87	0.74	0.86	0.27
THF/H <sub>2</sub> O (50/50)	0.50	0.97	0.75	0.84	0.70	0.88	– <sup>[b]</sup>
THF/H <sub>2</sub> O (75/25)	0.51	0.93	0.68	0.79	0.55	0.77	– <sup>[b]</sup>
MeCN	0.56	0.85	0.68	0.82	0.53	0.86	0.19
MeOH	0.46	0.93	0.66	0.81	0.48	0.74	– <sup>[b]</sup>
THF	0.43	0.81	0.06	0.67	0.30	0.85	– <sup>[b]</sup>

[a] Estimated error  $\pm 6\%$ . [b] No fluorescence quenching.

the extent of fluorescence quenching increases with solvent polarity, that is, forward electron transfer is accelerated with increasing solvent polarity. Thus, it can be excluded that forward electron transfer is responsible for the two reverse solvent effects, and back electron transfer, which is a key factor leading to low repair quantum yield of model compounds,<sup>[16]</sup> may be the factor controlling the two reverse solvent effects.

The free-energy change  $\Delta G$  for back electron transfer is the energy level of the charge-separated state ( $\text{Ch}^+ - \text{D}^-$ ), which can be estimated by using thermodynamic redox potentials. The free-energy difference between the charge-transfer state and the ground state is given by Equation (1):<sup>[17]</sup>

$$-\Delta G_{\text{bet}} = E_{\text{ox}} - E_{\text{red}} + \Delta E_{\text{coul}} \quad (1)$$

$$\Delta E_{\text{coul}}/\text{eV} = \frac{e}{4\pi\epsilon_0 a} \left( \frac{1}{\epsilon} - \frac{2}{37.5} \right) \quad (2)$$

where  $E_{\text{ox}}$  and  $E_{\text{red}}$  are potentials for one-electron oxidation of a donor (indole or its derivatives, Table 3)<sup>[18]</sup> and one-electron reduction of an acceptor (T < > T,  $-2.20$  V vs. SCE<sup>[19]</sup>), respectively;  $\Delta E_{\text{coul}}$  and  $\Delta E_{0,0}$  are the Coulomb term and the energy level of the excited state, respectively; the latter can be obtained from the fluorescence peaks of the indole T < > T model compounds in the corresponding solvents, and  $\epsilon$ ,  $a$  are the static dielectric constant of a solvent and the center-to-center distance between a donor and an acceptor, respectively.

Table 3 presents the peak oxidation potentials measured for each indole by linear sweep voltammetry (LSV).<sup>[18]</sup> Although the substituted positions are different for some model compounds, under the same conditions, the variation in the peak

Table 3. Oxidation potentials $E_{\text{ox}}$ , Hammett constants $\sigma$ , and changes in free energy $\Delta G_{\text{det}}$ of compounds <b>2a–2g</b> .				
Compound	Substituents	$E_{\text{ox}}^{\text{[a]}}$	$-\Delta G_{\text{det}}$ (MeCN)	$\sigma^{\text{[b]}}$
<b>2a</b>	5-OMe	0.83	2.97	$-0.268$ ( <i>p</i> )
<b>2b</b>	2,3-Me <sub>2</sub>	0.90 <sup>[c]</sup>	3.04	$-0.239$ ( <i>p</i> + <i>m</i> )
<b>2c</b>	3-Me	0.94	3.08	$-0.069$ ( <i>m</i> )
<b>2d</b>	H	1.10	3.24	0
<b>2e</b>	5-Br	1.10	3.24	0.232 ( <i>p</i> )
<b>2f</b>	6-Cl	1.30	3.44	0.373 ( <i>m</i> )
<b>2g</b>	4-CN	1.64	3.78	0.56 ( <i>m</i> )

[a] From ref. [17]. [b] From ref. [19], *p* and *m* denote *para* and *meta* substituent, respectively. [c]  $E_{\text{ox}}$  of 2,3-dimethylindole estimated.

oxidation potential should mirror changes in the oxidation potential. With increasing oxidation potential, from 0.83 eV for methoxyindole to 1.64 eV for cyanoindole, the value of  $-\Delta G_{\text{det}}$  increases, which is favorable for back electron transfer and leads to the quantum yields of  $T < > T$  splitting decreasing in the sequence from **2a** to **2g** in acetonitrile. The variational trend in other solvents is identical.

The data in Table 3 also show that the splitting efficiency of indole  $T < > T$  model **2d** is affected by the substituents at the indole ring. These effects are often quantified by means of substituent constants, which were first introduced by Hammett.<sup>[20]</sup> There are two  $\sigma$  values for each substituent relative to the nitrogen atom of the indole ring, whereby R1 and R4 are *para* substituents, and R2, R3, and R5 *meta* substituents. The  $\sigma$  value of model **2b** is the sum of *para* and *meta* values. Although the  $\sigma$  values vary with the solvents, this variation is usually small enough to be ignored. Reaction rates for a substituted molecule relative to the rate for an unsubstituted molecule are plotted against the Hammett constants in order to gain insight into the reaction mechanism. Thus, in the present  $T < > T$ -splitting reaction, we can relate the splitting quantum yields to the Hammett constants, as the logarithm of  $\Phi$  is a function of the free energy of activation. These relations can be exploited to deduce the mechanism of the  $T < > T$ -splitting reaction.

In Figure 3, the logarithm of the ratio of the measured  $\Phi$  for the substituted and unsubstituted indole- $T < > T$  is plotted against the Hammett parameter from ref. [20b]. The Hammett plots are linear correlations with  $\rho$  values of  $-0.20$  ( $r=0.87$ ),  $-0.69$  ( $r=0.92$ ),  $-1.57$  ( $r=0.95$ ),  $-1.98$  ( $r=0.95$ ),  $-2.39$  ( $r=0.95$ ), and  $-2.46$  ( $r=0.90$ ) in THF/H<sub>2</sub>O (10/90), THF/H<sub>2</sub>O (25/75), THF/H<sub>2</sub>O (50/50), THF/H<sub>2</sub>O (75/25), acetonitrile, and THF respectively. Figure 3 shows a clear trend in that the slope of the Hammett plot becomes more negative as the solvent polarity decreases. This negative slope indicates that the indole moiety in the  $T < > T$ -splitting reaction is positively charged (or loses negative charge), which corresponds with the indole radical cation of the electron-transfer reaction. Moreover, with decreasing solvent polarity, the negative  $\rho$  value increases gradually, and this implies that the repair reaction is more sensitive to substituents in low-polarity solvents.

The reaction constant  $\rho$  has been interpreted as a measure of the susceptibility to substituent effects of the charge-sepa-

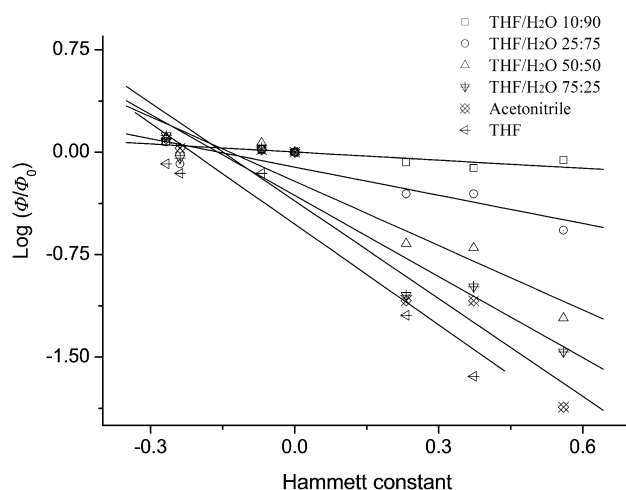


Figure 3. Plot of the splitting quantum yields  $\Phi$  of model compounds versus Hammett constants  $\sigma$  in various solvents.

rated state, leading a significant competition between  $T < > T$  splitting and futile back electron transfer. The larger  $\rho$  value in low-polarity solvents suggests more charge transfer in the charge-separated intermediate ( $X\text{-Ch}^+-\text{D}^-$ , where X denotes the substituted group). When X is an EDG, the zwitterion can be stabilized by charge delocalization, while an EWG leads to destabilizing effect. Thus, in low-polarity solvents, the EDGs of models **2a–2d** can delocalize the charge-separated intermediate and leave more time to cleave the  $T < > T$ , so that a high splitting efficiency results, whereas the EWGs of models **2e–2g** destabilize the intermediate and thus favor back electron transfer and inhibit  $T < > T$  splitting. Since solvent has a large effect on the magnitude of  $\rho$ , the  $\rho$  value clearly decreases with increasing solvent polarity. In high-polarity solvents, the small  $\rho$  value implies that there is less charge transfer in the charge-separated state and the reaction rate is almost unaffected by substituent effects, because solvation effects in high-polarity solvents can decrease the charge delocalization of EDGs or the destabilization of EWGs, which leads to decreased splitting efficiency of models **2a–2d** and increased splitting efficiency of models **2e–2g** in high-polarity solvents. Therefore, the EDGs of models **2a–2d** can stabilize the charge-separated state by charge delocalization, and the larger  $\rho$  value in low-polarity solvents makes the intermediate more stable, which leads to higher splitting quantum yields in low-polarity solvent. Conversely, the EWGs of models **2e–2g** favor destabilization of the charge-separated state, and high-polarity solvents decrease the destabilization, and hence splitting is more efficient in high-polarity solvents.

### 3. Conclusions

We have measured the splitting quantum yields of a series of substituted indole- $T < > T$  model compounds with a short linker **2a–2g** and observed two reverse solvent effects: an increase in splitting efficiency in solvents of lower polarity for models **2a–2d** with an EDG and faster splitting in higher polarity solvents for models **2e–2g** with an EWG. According to

the Hammett equation, the negative value of the slope of the Hammett plot indicates that the indole moiety loses negative charge during the T < > T-splitting reaction, and the larger negative value implies that the repair reaction is more sensitive to substituent effects in low-polarity solvents. The EDGs of models **2a–2d** can delocalize the charge-separated state and low-polarity solvents make it more stable, which leads to higher splitting efficiency in low-polarity solvents. Conversely, the EWGs of models **2e–2g** favor destabilization of the charge-separated state and high-polarity solvents decrease the destabilization, and hence splitting is more efficient in high-polarity solvents. Analysis of solvent effects and substituent effects on the charge-separated state can interpret the two reverse solvent effects on the splitting efficiency. It can be deduced that the repair efficiency in CPD photolyase can be increased by tuning the solvent polarity<sup>[4]</sup> and the redox potential of the flavoproteins,<sup>[21]</sup> and this work helps us to screen more efficient photosensitizers based on structure optimization.

## Experimental Section

**General:** Melting points are uncorrected. All materials were obtained from commercial suppliers and used as received. Solvents of technical quality were distilled prior to use. DMF was dried overnight with K<sub>2</sub>CO<sub>3</sub> and distilled. THF was dried with sodium metal and distilled before use for the photosplitting measurements on the model compounds. Acetonitrile and methanol were of spectroscopic grade from commercial suppliers and used without further purification.

**Measurement of Steady-State Fluorescence Emission:** Fluorescence emission spectra were measured at room temperature on a fluorescence spectrometer. To determine the extent of fluorescence quenching *Q*, the fluorescence intensities *F*<sub>indole-D</sub> of **2a–2g** were compared to that (*F*<sub>indole</sub>) of the corresponding indole without an attached T < > T (**4a–4g**, see the Supporting Information), that is,  $Q = 1 - F_{\text{indole-D}}/F_{\text{indole}}$ . The concentrations of the indole moiety of the indole-T < > T models and the free indole were controlled within 0.05 for absorbance at the corresponding excitation wavelength and the fluorescence intensities were normalized with the absorbances.

**Measurement of Splitting Quantum Yields of Model Compounds:** To measure the quantum yields of T < > T splitting of the model compounds [ $\Phi = (\text{rate of T < > T splitting})/(\text{rate of photons absorbed})$ ], sample solutions ( $\approx 5 \times 10^{-5}$  M, 3 mL) were prepared and placed in quartz cuvettes with a Teflon stopper and then irradiated with light of the corresponding wavelength (295 nm for **2d**, 310 nm for **2a**, 320 nm for **2g**, 300 nm for **2b**, **2c**, **2e**, **2f**) from a fluorescence spectrometer operated with a 10 nm slit. The absorbances at 273 nm (*A*<sub>273</sub>) and the corresponding wavelength (*A*<sub>ex</sub>) were recorded at certain intervals of time after irradiation. The extent of T < > T splitting was measured by monitoring the increase in *A*<sub>273</sub> due to regeneration of the thymine bases. The *A*<sub>273</sub> change ( $\Delta A_{273}$ ) of the solution depends on the extent of splitting of the model compounds. The plot of  $\Delta A_{273}$  against irradiation time (*t*/min) is well fitted as a straight line, whereby the slope of the straight line *B* reflects the splitting rate of the model compound. The intensity of the excitation light beam (*I*<sub>0</sub>, unit: einstein min<sup>-1</sup>) was measured by ferrioxalate actinometry.<sup>[22]</sup> The intensity of light absorbed (*I*<sub>a</sub>) by the solution was calculated in terms of

Beer's law,  $I_a = I_0(1 - 10^{-A_{ex}})$ . The change in the molar extinction coefficients ( $\Delta \epsilon_{273}$ ) was obtained from the UV absorption spectra of the model compounds and the fully split products. These values allowed calculation of the quantum yield,  $\Phi = BV_0/\Delta \epsilon_{273}I_a$ , wherein *V*<sub>0</sub> is the volume of irradiation solution ( $3 \times 10^{-3}$  L). The experimental error was within 10%.

The quantum yields of splitting did not significantly change with and without N<sub>2</sub> bubbling prior to irradiation. Hence, nondeaerated solutions were employed in all measurements of the quantum yield. To limit the competition for absorption of the irradiated light between model compounds and photoproducts, the splitting extent of the model compounds was controlled within 10% in all of the measurements of the quantum yield.

**General Method for the Synthesis of 2a–2g (Scheme 2):** A mixture of the appropriate indole or its derivative, 1,3-dibromopropane (15.0 equiv), 50% NaOH aqueous solution (10 mL), and TBAB (7.2 equiv) in 20 mL of toluene was stirred at room temperature for 3.5 h. The mixture was diluted with water and extracted with EtOAc. The organic layers were dried with Na<sub>2</sub>SO<sub>4</sub>, filtered, and concentrated in vacuo. The 3-(1-bromopropyl)indole derivatives **1a–1g** were obtained as oils after purification by column chromatography on silica gel. Then, sodium *tert*-butoxide (2.0 equiv) was added to a solution of *cis-syn* thymine dimer **5** (62 mg, 0.20 mmol) in 5 mL of DMF and the reaction mixture stirred at room temperature for 30 min. The above oils **1a–1g** (2.0 equiv) were added, and stirring was resumed at room temperature for 3 h. The mixture was diluted with water and extracted with EtOAc. The organic layer was dried with Na<sub>2</sub>SO<sub>4</sub>, filtered, and concentrated in vacuo. The crude product was purified by flash chromatography and recrystallization. The products were obtained as white powders.

**Model Compound 2a:** By the above procedure, **1a** (1.8 g, 78%) was obtained as light yellow oil. **2a** (54 mg, 55%) was prepared from **1a** and **5** and purified by column chromatography on silica gel (EtOAc as eluent) as a white powder. M.p. 252–253 °C; <sup>1</sup>H NMR (300 MHz, CDCl<sub>3</sub>):  $\delta = 1.32$  (s, 3H, CH<sub>3</sub>), 1.41 (s, 3H, CH<sub>3</sub>), 1.64–1.67 (m, 1H), 2.01–2.17 (m, 2H), 2.27–2.39 (m, 2H), 2.80 (s, 3H, NCH<sub>3</sub>), 3.46 (d, *J* = 7.1 Hz, 1H, CH), 3.60 (d, *J* = 7.1 Hz, 1H, CH), 3.85 (s, 3H, OCH<sub>3</sub>), 3.91–3.96 (m, 2H), 4.02–4.27 (m, 5H), 6.43–7.26 ppm (m, 5H, ArH); <sup>13</sup>C NMR (75 MHz, CDCl<sub>3</sub>):  $\delta = 18.3$  (CH<sub>3</sub>), 18.7 (CH<sub>3</sub>), 22.9, 28.8, 36.5, 41.7, 41.8, 44.1, 46.2, 50.7 (C), 51.0 (C), 56.1 (OCH<sub>3</sub>), 59.0 (CH), 60.7 (CH), 101.5, 103.0, 110.1, 112.4, 128.4, 129.3, 131.3, 151.9, 152.0, 154.4, 170.1, 170.2 ppm; HRMS (ESI-TOF) calcd for C<sub>26</sub>H<sub>32</sub>N<sub>5</sub>O<sub>3</sub> [M+H]<sup>+</sup>: 494.2415, found: 494.2398.

**Model Compound 2b:** By the above procedure, **1b** (450 mg, 25%) was obtained as light yellow oil. **2b** (70 mg, 71%) was prepared from **1b** and **5** and purified by column chromatography on silica gel (petroleum ether/EtOAc 4/1 → 1/1 as eluent) as a white powder. M.p. 258–259 °C; <sup>1</sup>H NMR (300 MHz, CDCl<sub>3</sub>):  $\delta = 1.34$  (s, 3H, CH<sub>3</sub>), 1.40 (s, 3H, CH<sub>3</sub>), 1.62 (m, 1H), 1.83–2.13 (m, 2H), 2.25 (s, 3H, CH<sub>3</sub>), 2.28–2.29 (m, 1H), 2.33 (s, 3H, CH<sub>3</sub>), 2.36–2.42 (m, 1H), 2.76 (s, 3H, NCH<sub>3</sub>), 3.36 (d, *J* = 7.1 Hz, 1H, CH), 3.46 (d, *J* = 7.1 Hz, 1H, CH), 3.91–3.95 (m, 2H), 4.02–4.27 (m, 5H), 7.07–7.51 ppm (m, 4H, ArH); <sup>13</sup>C NMR (75 MHz, CDCl<sub>3</sub>):  $\delta = 9.0$  (CH<sub>3</sub>), 10.4 (CH<sub>3</sub>), 18.3 (CH<sub>3</sub>), 18.6 (CH<sub>3</sub>), 22.9, 29.3, 36.3, 40.7, 41.7, 41.8, 45.8, 50.7 (C), 50.8 (C), 58.6 (CH), 60.6 (CH), 107.4, 108.7, 118.4, 119.1, 121.0, 128.9, 132.1, 136.0, 151.9 (2C), 170.1, 170.2 ppm; HRMS (ESI-TOF) calcd for C<sub>27</sub>H<sub>34</sub>N<sub>5</sub>O<sub>4</sub> [M+H]<sup>+</sup>: 492.262, found 492.2605.

**Model Compound 2c:** By the above procedure, **1c** (1.8 g, 79%) was obtained as colorless oil. **2c** (60 mg, 63%) was prepared from **1c** and **5** and purified by column chromatography on silica gel (EtOAc as eluent) as a white amorphous powder. M.p. 260–263 °C;

$^1\text{H}$  NMR (300 MHz,  $\text{CDCl}_3$ ):  $\delta$  = 1.27 (s, 3H,  $\text{CH}_3$ ), 1.40 (s, 3H,  $\text{CH}_3$ ), 1.62–1.63 (m, 1H), 2.01–2.03 (m, 1H), 2.14–2.16 (m, 1H), 2.31 (s, 3H,  $\text{CH}_3$ ), 2.33–2.40 (m, 2H), 2.79 (s, 3H,  $\text{NCH}_3$ ), 3.41 (d,  $J$  = 7.1 Hz, 1H, CH), 3.54 (d,  $J$  = 7.1 Hz, 1H, CH), 3.92–3.96 (m, 2H), 4.05–4.27 (m, 5H), 6.85–7.62 ppm (m, 5H, ArH);  $^{13}\text{C}$  NMR (75 MHz,  $\text{CDCl}_3$ ):  $\delta$  = 9.8 ( $\text{CH}_3$ ), 18.2 ( $\text{CH}_3$ ), 18.7 ( $\text{CH}_3$ ), 22.9, 28.8, 36.4, 41.7, 41.8, 43.7, 46.1, 50.7 (C), 51.0 (C), 58.8 (CH), 60.7 (CH), 109.2, 111.1, 119.1, 119.5, 121.9, 125.4, 129.1, 136.3, 151.8, 152.0, 170.1, 170.2 ppm; HRMS (ESI-TOF) calcd for  $\text{C}_{26}\text{H}_{32}\text{N}_5\text{O}_4$   $[M+H]^+$ : 478.2467, found: 478.2449.

Model Compound **2d**:<sup>[11]</sup> By the above procedure, **1d** (1.67 g, 82%) was obtained as light yellow oil. **2d** (60 mg, 65%) was prepared from **1d** and **5** and purified by column chromatography on silica gel (EtOAc/MeOH 1/0→5/1 as eluent) as a white amorphous powder. M.p. 244–247 °C; HRMS (ESI-TOF) calculated for  $\text{C}_{25}\text{H}_{30}\text{N}_5\text{O}_4$   $[M+H]^+$ : 464.2304, found: 464.2292.

Model Compound **2e**: By the above procedure, **1e** (630 mg, 80%) was obtained as light yellow oil. **2e** (43 mg, 41%) was prepared from **1e** and **5** and purified by column chromatography on silica gel (petroleum ether/EtOAc 1/3 as eluent) as a white powder. M.p. 237–238 °C;  $^1\text{H}$  NMR (300 MHz,  $\text{CDCl}_3$ ):  $\delta$  = 1.36 (s, 3H,  $\text{CH}_3$ ), 1.44 (s, 3H,  $\text{CH}_3$ ), 1.63–1.68 (m, 1H), 2.01–2.18 (m, 2H), 2.27–2.39 (m, 2H), 2.82 (s, 3H,  $\text{NCH}_3$ ), 3.53 (d,  $J$  = 7.1 Hz, 1H, CH), 3.66 (d,  $J$  = 7.1 Hz, 1H, CH), 3.91–3.98 (m, 2H), 4.04–4.27 (m, 5H), 6.46 (d, 1H, ArH), 7.09–7.77 ppm (m, 4H, ArH);  $^{13}\text{C}$  NMR (75 MHz,  $\text{CDCl}_3$ ):  $\delta$  = 17.4 ( $\text{CH}_3$ ), 17.6 ( $\text{CH}_3$ ), 22.1, 28.0, 35.5, 40.5, 40.8, 43.2, 44.9, 50.0 (C), 50.2 (C), 57.4 (CH), 59.2 (CH), 100.2, 111.4, 111.6, 122.5, 123.3, 129.7, 129.8, 134.2, 151.2, 151.3, 169.8, 169.9 ppm; HRMS (ESI-TOF) calculated for  $\text{C}_{25}\text{H}_{29}\text{BrN}_5\text{O}_4$   $[M+H]^+$ : 542.1395, found: 542.1397.

Model Compound **2f**: By the above procedure, **1f** (1.8 g, 78%) was obtained as light yellow oil. **2f** (60 mg, 60%) was prepared from **1f** and **5** and purified by column chromatography on silica gel (EtOAc as eluent) as a white powder. M.p. 245–247 °C;  $^1\text{H}$  NMR (300 MHz,  $\text{CDCl}_3$ ):  $\delta$  = 1.36 (s, 3H,  $\text{CH}_3$ ), 1.43 (s, 3H,  $\text{CH}_3$ ), 1.63–1.65 (m, 1H), 2.01–2.17 (m, 2H), 2.31–2.40 (m, 2H), 2.84 (s, 3H,  $\text{NCH}_3$ ), 3.55 (d,  $J$  = 7.1 Hz, 1H, CH), 3.65 (d,  $J$  = 7.1 Hz, 1H, CH), 3.92–3.97 (m, 2H), 4.03–4.28 (m, 5H), 6.48–7.56 ppm (m, 5H, ArH);  $^{13}\text{C}$  NMR (75 MHz,  $\text{CDCl}_3$ ):  $\delta$  = 18.3 ( $\text{CH}_3$ ), 18.7 ( $\text{CH}_3$ ), 22.8, 30.5, 41.7, 41.8, 44.0, 46.1, 50.7 (C), 51.0 (C), 59.1 (CH), 60.7 (CH), 102.2, 109.4, 120.5, 122.3, 127.4, 128.0, 128.6, 136.3, 151.8, 152.1, 170.1 ppm (2C); HRMS (ESI-TOF) calcd for  $\text{C}_{25}\text{H}_{29}\text{ClN}_5\text{O}_4$   $[M+H]^+$ : 498.1904, found: 498.1903.

Model Compound **2g**: By the procedure above, **1g** (400 mg, 86%) was obtained as light yellow oil. **2g** (40 mg, 41%) was prepared from **1g** and **5** and purified by column chromatography on silica gel (EtOAc as eluent) as a white powder. M.p. 268–270 °C;  $^1\text{H}$  NMR (300 MHz,  $\text{CDCl}_3$ ):  $\delta$  = 1.41 (s, 3H,  $\text{CH}_3$ ), 1.46 (s, 3H,  $\text{CH}_3$ ), 1.66 (m, 1H), 2.04–2.19 (m, 2H), 2.32–2.41 (m, 2H), 2.84 (s, 3H,  $\text{NCH}_3$ ), 3.62 (d,  $J$  = 7.0 Hz, 1H, CH), 3.74 (d,  $J$  = 7.0 Hz, 1H, CH), 3.93–3.98 (m, 2H), 4.11–4.28 (m, 5H), 6.74–7.55 ppm (m, 5H, ArH);  $^{13}\text{C}$  NMR (75 MHz,  $\text{CDCl}_3$ ):  $\delta$  = 17.4 ( $\text{CH}_3$ ), 17.7 ( $\text{CH}_3$ ), 22.2, 28.2, 35.7, 40.7, 41.0, 43.4, 44.9, 50.1 (C), 50.4 (C), 57.3 (CH), 59.2 (CH), 99.0, 101.5, 115.4, 118.6, 121.0, 124.7, 128.9, 132.0, 135.3, 151.4, 151.5, 170.1, 170.2 ppm; HRMS (ESI-TOF) calcd for  $\text{C}_{26}\text{H}_{29}\text{N}_6\text{O}_4$   $[M+H]^+$ : 489.2247, found: 489.2245.

## Acknowledgements

The authors are grateful for the financial support by the National Natural Science Foundation of China (Grant Nos. 20802003 and

30870581), Anhui Province and China Postdoctoral Science Foundation (Grant No. 20100470823).

**Keywords:** DNA photorepair • electron transfer • photochemistry • solvent effects • substituent effects

- [1] E. C. Friedberg, G. C. Walker, W. Siede, *DNA Repair and Mutagenesis*, ASM, Washington, DC, 1995.
- [2] K. M. Lima-Bessa, C. F. M. Menck, *Curr. Biol.* **2005**, *15*, R58–R61.
- [3] A. Sancar, *Chem. Rev.* **2003**, *103*, 2203–2237.
- [4] a) Y.-T. Kao, C. L. Saxena, J. Wang, A. Sancar, D. Zhong, *Proc. Natl. Acad. Sci. USA* **2005**, *102*, 16128–16132; b) Z. Liu, C. Tan, X. Guo, Y.-T. Kao, J. Li, L. Wang, A. Sancar, D. Zhong, *Proc. Natl. Acad. Sci. USA* **2011**, *108*, 14831–14836; c) V. Thiagarajan, M. Byrdin, A. P. Eker, P. Müller, K. Brettel, *Proc. Natl. Acad. Sci. USA* **2011**, *108*, 9402–9407.
- [5] a) F. Masson, T. Laino, U. Rothlisberger, J. Hutter, *ChemPhysChem* **2009**, *10*, 400–410; b) A. A. Hassanali, D. Zhong, S. J. Singer, *J. Phys. Chem. B* **2011**, *115*, 3848–3859.
- [6] P. F. Heelis, R. F. Hartman, S. D. Rose, *Chem. Soc. Rev.* **1995**, *24*, 289–297.
- [7] K. Heil, D. Pearson, T. Carell, *Chem. Soc. Rev.* **2011**, *40*, 4271–4278.
- [8] K. Brettel, M. Byrdin, *Curr. Opin. Struct. Biol.* **2010**, *20*, 693–701.
- [9] a) S.-T. Kim, R. F. Hartman, S. D. Rose, *Photochem. Photobiol.* **1990**, *52*, 789–794; b) S.-T. Kim, S. D. Rose, *J. Photochem. Photobiol. B* **1992**, *12*, 179–191; c) D. G. Hartzfeld, S. D. Rose, *J. Am. Chem. Soc.* **1993**, *115*, 850–854.
- [10] a) R. Epple, E.-U. Wallenborn, T. Carell, *J. Am. Chem. Soc.* **1997**, *119*, 7440–7451; b) J. Butenandt, A. P. Eker, T. Carell, *Chem. Eur. J.* **1998**, *4*, 642–654; c) T. Carell, R. Epple, *Eur. J. Org. Chem.* **1998**, 1245–1258; d) R. Epple, T. Carell, *Angew. Chem.* **1998**, *110*, 986–989; *Angew. Chem. Int. Ed.* **1998**, *37*, 938–941; e) R. Epple, T. Carell, *J. Am. Chem. Soc.* **1999**, *121*, 7318–7329; f) J. Butenandt, L. T. Burgdorf, T. Carell, *Angew. Chem.* **1999**, *111*, 718–721; *Angew. Chem. Int. Ed.* **1999**, *38*, 708–711; g) J. Butenandt, R. Epple, E.-U. Wallenborn, A. P. Eker, E.-U. Gramlich, T. Carell, *Chem. Eur. J.* **2000**, *6*, 62–72; h) M. K. Cichon, S. Arnold, T. Carell, *Angew. Chem.* **2002**, *114*, 793–796; *Angew. Chem. Int. Ed.* **2002**, *41*, 767–770; i) Q. H. Song, W. J. Tang, X. M. Hei, H. B. Wang, Q. X. Guo, S. Q. Yu, *Eur. J. Org. Chem.* **2005**, 1097–1106; j) S. Breger, M. Meltzer, U. Hennecke, T. Carell, *Chem. Eur. J.* **2006**, *12*, 6469–6477.
- [11] W. J. Tang, Q. X. Guo, Q. H. Song, *J. Phys. Chem. B* **2009**, *113*, 7205–7210.
- [12] a) Q. Q. Wu, Q. H. Song, *J. Phys. Chem. B* **2010**, *114*, 9827–9832; b) H. M. Zhou, W. J. Tang, H. Zhang, X. X. Li, J. Li, *J. Photochem. Photobiol. A* **2012**, *246*, 60–66.
- [13] T. Carell, R. Epple, V. Gramlich, *Helv. Chim. Acta* **1997**, *80*, 2191–2203.
- [14] K. Fukui, T. Yonezawa, H. Shingu, *J. Chem. Phys.* **1952**, *20*, 722–725.
- [15] a) Q. H. Song, H. B. Wang, W. J. Tang, Q. X. Guo, S. Q. Yu, *Org. Biomol. Chem.* **2006**, *4*, 291–298; b) W. J. Tang, Q. H. Song, H. B. Wang, J. Y. Yu, Q. X. Guo, *Org. Biomol. Chem.* **2006**, *4*, 2575–2580; c) Q. H. Song, W. J. Tang, X. B. Ji, H. B. Wang, Q. X. Guo, *Chem. Eur. J.* **2007**, *13*, 7762–7770.
- [16] Y.-T. Kao, Q. H. Song, C. Saxena, L. Wang, D. Zhong, *J. Am. Chem. Soc.* **2012**, *134*, 1501–1503.
- [17] A. A. Weller, *Z. Phys. Chem.* **1982**, *133*, 93–98.
- [18] P. Jennings, A. C. Jones, A. R. Mount, A. D. Thomson, *J. Chem. Soc. Faraday Trans.* **1997**, *93*, 3791–3797.
- [19] M. R. Scannell, D. J. Fenick, S. R. Yeh, D. E. Falvey, *J. Am. Chem. Soc.* **1997**, *119*, 1971–1977.
- [20] a) L. P. Hammett, *J. Am. Chem. Soc.* **1937**, *59*, 96–103; b) C. Hansch, A. Leo, R. W. Taft, *Chem. Rev.* **1991**, *91*, 165–195.
- [21] a) A. Mees, T. Klar, P. Gnau, U. Hennecke, A. P. Eker, T. Carell, L.-O. Essen, *Science* **2004**, *306*, 1789–1793; b) Y. M. Gindt, J. P. Schelvis, K. L. Thoren, T. H. Huang, *J. Am. Chem. Soc.* **2005**, *127*, 10472–10473.
- [22] S. L. Murov, I. Carmichael, G. L. Hug, *Handbook of Photochemistry*, 2nd ed., Marcel Dekker, New York, 1993.

Received: August 10, 2012

Published online on October 4, 2012